

Dyes and Pigments

journal homepage: www.elsevier.com/locate/dyepig

Exploring the excited-states of squaraine dyes with TD-DFT, SOS-CIS(D) and ADC(2)

Fadel Bassal ^a, Adèle D. Laurent ^a, Boris Le Guennic ^b, Denis Jacquemin ^{a, c, *}

^a Laboratoire CEISAM - UMR CNRS 6230, Université de Nantes, 2 Rue de la Houssinière, BP 92208, 44322 Nantes Cedex 3, France

^b Institut des Sciences Chimiques de Rennes, UMR 6226 CNRS-Université de Rennes 1, 263 Av. du Général Leclerc, 35042 Rennes Cedex, France

^c Institut Universitaire de France, 1, Rue Descartes, F-75231 Paris Cedex 05, France

ARTICLE INFO

Article history:

Received 27 October 2016

Received in revised form

20 November 2016

Accepted 21 November 2016

Available online 27 November 2016

Keywords:

Optical spectra

Cyanine dyes

Ab initio calculations

TD-DFT

Fluorescence

ABSTRACT

We investigate the electronic excited-states of a large panel of squaraine derivatives with first principles tools taking into account environmental effects, with a focus on 0–0 energies and band shapes. First we show that while TD-DFT yields significantly too large 0–0 energies, correcting the TD-DFT values with ADC(2) provides much more accurate estimates. Second, though the geometric relaxation after photon absorption is limited, this investigation also indicates that using theoretical vertical estimates to approximate the experimental 0–0 energies is not a very appealing approach. In contrast, for experimentally non-fluorescent compounds one can use the measured λ_{max} as an approximation of the 0–0 energy with a minimal loss of accuracy. The proposed computational approach delivers a ca. 0.125 eV accuracy for a large number of compounds and therefore stands as one of the first robust method to predict the optical spectra of this important class of dyes. We also investigate the band shapes of selected derivatives and show that TD-DFT vibronic couplings allow an accurate reproduction of the experimental topologies of both absorption and emission bands.

© 2016 Elsevier Ltd. All rights reserved.

1. Introduction

Squaraines (SQs) constitute an important class of organic dyes. They are known for their strong and intense absorption of light as well as their structural diversity, as various substituents can be added through organic synthesis in order to tune their optical properties [1–14]. These molecules are generally obtained by condensation of squaric acid with electron rich aromatic molecules, e.g., *N,N*-dialkylanilines, pyrroles, indoles, quinaldine, indolizine, benzothiazoles, azulenes, quinolones ... and the resulting compounds typically show absorption at wavelengths going up to the near-infrared region. As their names imply, SQs present a core constituted of a four-member sp^2 -carbon π -conjugated cycle often substituted by two oxygen atoms and two π -conjugated moieties. In one of the possible limit mesomeric forms, the SQ core is positively charged – the two oxygen atoms bearing the negative charge – and this positive charge can be viewed as delocalized over the odd number of carbon atoms constituting the π -conjugated

pathway. Therefore, SQ dyes present similarities with the traditional merocyanine dyes [15]. From another point of view, one can state that the electron-deficient square core acts as a strong acceptor whereas the electron-rich arms act as donors so that these dyes present a D–A–D quadrupolar charge-transfer (CT) structure. These very specific electronic features have made SQs valuable building blocks in numerous fields, e.g., bio-imaging [16–18], photodynamic therapy [19–25], electrophotography [26,27], organic light-emitting diodes [28,29], sensors [30,31], solar cells [32–34], and non-linear optical materials [35–37].

Unsurprisingly, SQs have also been the subject of several computational investigations. To the best of our knowledge, the first theoretical study, dating back from 1986, is due to Bigelow and Freund [38]. Using the MNDO and CNDO/S(S + DESC) semi-empirical approaches, they characterized both the ground-state (GS) and the lowest excited-state (ES) of a prototypical SQ dye. These early calculations already demonstrated that the color of SQs is related to a state presenting a blend of cyanine and charge-transfer characters [38]. A decade latter, the initial first principle calculations on SQs appeared. In 2009, Geiger and coworkers performed gas-phase Density Functional Theory (DFT) and Time-Dependent DFT (TD-DFT) calculations of two SQ dyes used in solar cells [39]. They

* Corresponding author. Laboratoire CEISAM – UMR CNRS 6230, Université de Nantes, 2 Rue de la Houssinière, BP 92208, 44322 Nantes Cedex 3, France.

BLYP, BPW91, PBE, B3LYP, PBEO, and X3LYP, and surprisingly found a better match with experiment when using pure XCFs rather than hybrid XCFs [39]. The same year, Russo's group considered the first significant panel of symmetric SQs dyes and used both TD-DFT and CC2 to explore their ES [40]. They found that the atomic basis set effects were small at both levels of theories and that the transition energies obtained with the two methods show quite large errors (~0.3 eV), with a significant overestimation of the transition energies for TD-DFT that yields too blueshifted λ_{max} . These outcomes are indicative of a significant cyanine-character of the excited-state [41], as the transition energies of CT ES are generally underestimated (and not overestimated) by TD-DFT [42,43]. More recently, the same group investigated the ES of six SQs using three functionals (PBEO, M06, and ω B97X-D) in a study focusing on the singlet-triplet splittings and spin-orbit couplings [44]. Besides a good agreement with experimental X-ray structures [45], the authors reported a good match between M06 and experimental optical data, though the above-mentioned blueshifts pertain [44]. In another recent work, TD-DFT transition energies determined with a large panel of functionals were compared to both SAC-CI values and experimental results for several SQs; the wavefunction method emerging as more accurate than the density-based one [46]. Eventually, the only investigation to date that went beyond the frozen GS geometry approach is due to Liu and coworkers [47]. They determined the ES geometries and vertical emission energies of four SQ dyes in four solvents using a continuum model to describe the environmental effects. One can also find other more specific TD-DFT investigations of SQs in the literature [48–51].

Despite these earlier useful theoretical works, there is, to the best of our knowledge, no investigation of the band shapes nor 0-0 energies of SQ derivatives. In contrast to the vertical estimates determined up to now (see above), these two properties allow direct and physically meaningful comparisons with experiment [52]. Indeed, the former can be straightforwardly compared to the measured absorption and fluorescence spectra if proper normalization is carried out [53], whereas the 0-0 energies correspond to the experimental absorption-fluorescence crossing point (AFCP) [54,55]. However, the determination of these two properties require the calculation of the ES Hessian, which remains computationally expensive, as well as of the vibronic couplings for the band shapes. We perform such task in this paper. Indeed we treat a very large number of SQs and determine 0-0 transition energies and compare them to available experimental data. The solvent effects are taken into account at all calculations steps by a refined continuum model [56,57], whereas several first principle methods are used. Indeed, we applied TD-DFT but also the second-order Algebraic-Diagrammatic Construction approach, ADC(2) [58], as well as the Scaled Opposite Spin version of Configuration Interaction Singles with a Double correction, namely SOS-CIS(D) [59].

2. Computational details

The general computational approach followed here has been detailed elsewhere [41,60], so that we only briefly outline it here. In this protocol, the structures and vibrational spectra are determined with TD-DFT, the solvent effects with the Polarizable Continuum Model (PCM) whereas the total and transition energies are computed with TD-DFT as well as electron-correlated wavefunction approaches. This protocol that allows to access accurate 0-0 energies at a reasonable computational cost even for rather large compounds was shown to be successful for several cyanine-like compounds (see Ref. [41] and references therein).

integration grid (so-called *ultrafine* grid). We applied the Berny-GEDIIS algorithm during the force-minimization process imposing a threshold of 10^{-5} a.u. on the residual mean forces. Point group symmetry was used when possible in order to lighten the computational burden that can be important for the computation of the TD-DFT Hessian. The GS equilibrium geometry of all investigated dyes was fully optimized at the DFT level using the M06-2X hybrid exchange-correlation functional [62,63] and the 6-31G(d) atomic basis set. It was checked by vibrational frequency calculations performed at the same level of theory that all structures are true minima of the potential energy surfaces. This choice of M06-2X is justified by numerous previous benchmarks [55,64–66], demonstrating the ability of this XCF to reproduce the ES trends in a wide range of organic compounds. The ES structures have been optimized at the same level of theory, using TD-DFT, and the numerical ES Hessian was systematically computed to ascertain the nature of the stationary point, as well as to obtain the zero-point vibrational energies (ZPVE) of the ES. The total and transition energies were computed on these GS and ES structures using the same XCF but selecting a much more extended atomic basis set, namely 6-311+G(2d,p).

Solvent effects have been included in the DFT and TD-DFT calculations by using the well-known Polarizable Continuum Model (PCM) [56] as implemented in Gaussian09. For both the ES geometry optimizations and Hessian calculations, we applied the linear-response (LR) PCM approach [67,68], whereas the ES total and transition energies have been determined within the corrected LR scheme (cLR) [57]. We applied the equilibrium PCM limit during the structural and vibrational calculations. We have determined both the absorption and emission energies in both the non-equilibrium and equilibrium limits. The differences between these two limits were found to be trifling (~0.001 eV) for the SQ dyes treated here. Default PCM radii and cavities were used.

In a second step, two wavefunction approaches have been employed to improve the TD-DFT transition energies. The first is the second-order ADC method, ADC(2) [58], that employs a diagrammatic perturbation expansion of the polarization propagator based on the Møller-Plesset partition of the Hamiltonian. The second is the more computationally effective SOS-CIS(D) approach [59], that was shown particularly successful for BODIPY derivatives [69]. The ADC(2) and SOS-CIS(D) calculations were performed with the Turbomole [70] and Q-Chem [71] packages, respectively, applying the resolution-of-identity (RI) technique to speed-up the calculations. The SOS-CIS(D) calculations were performed with the 6-311+G(2d,p) atomic basis set whereas the ADC(2) calculations used the aug-cc-pVQZ atomic basis sets. These choices are justified by previous works [40,72].

Vibrationally resolved absorption and emission spectra within the harmonic approximation were computed using the FCclasses program and the Franck-Condon (FC) approximation using the TD-DFT vibrational signatures of the two states (so-called adiabatic Hessian approach) [53,73–75]. The reported spectra were simulated using a convoluting Gaussian function presenting a half width at half maximum (HWHM) that was adjusted to allow straightforward comparisons with experiments (0.04 eV). A maximal number of 25 overtones for each mode and 20 combination bands on each pair of modes were included in the calculation. The maximum number of integrals to be computed for each class (ca. 10^6) was set so to obtain a sufficiently large FC factor (> 0.95).

3. Results and discussion

both cases, though the systems have a π -delocalized nature, one can notice that the variations of electron density are principally localized on the SQ center and vicinal atoms. As expected, the external dimethylamino groups of the dyes on the right hand-side appear mainly in blue, that is, play the role of electron donors. More interestingly, though one generally considers the SQ core as an acceptor, one notes here that the two keto moieties are mainly loosing electron density (donor), whereas the two carbon atoms of the SQ core directly bonded to the side groups gain a large amount of electron density when going from the GS to the ES. By following the π -conjugated path connecting the two external nitrogen atoms, one notices a loss/gain on electron density on the odd/even atomic positions, a behavior very typical of cyanine derivatives [41,76]. To go further, we list in Fig. 2 selected geometrical parameters determined with (TD-)DFT for the GS and ES structures for the second compound of Fig. 1 (see Fig. S1 in the SI for the first molecule). Clearly, the quinoidal nature of the compound appears in the two electronic states. Globally the variations of the bond distances after absorption of photon are rather limited. Indeed, the only two bond length variations exceeding 0.005 Å are, on the one hand, the elongation of the CC bond in the SQ core and, on the other hand, the contraction of the bond separating this core from the side phenyl rings. The localization of these changes are consistent with the density difference plots displayed in Fig. 1. Interestingly the CO distance is almost constant in the GS and the ES. Similar results have been obtained for the other SQ derivative (see SI).

3.2. Comparison with experimental 0-0 energies and band shapes

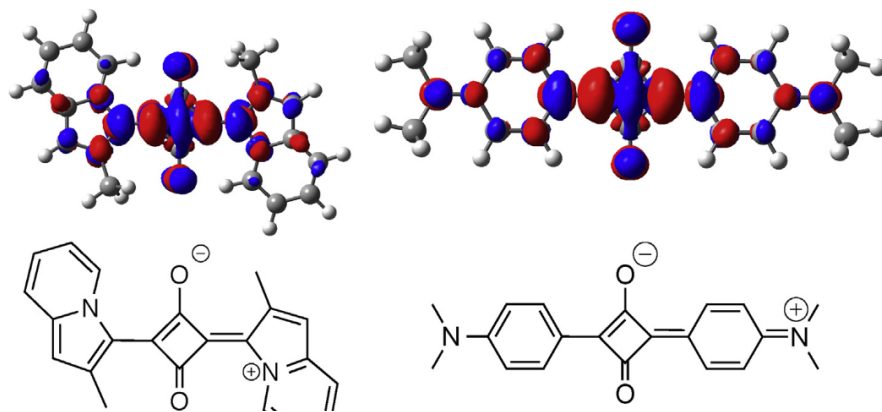
Let us now compare experimental and theoretical 0-0 energies for the twelve SQs displayed in Scheme 1. This set was selected not only to be representative of the molecular diversity of this class of dyes, but also because experimental fluorescence spectra have been measured for these molecules, allowing us to determine AFCP energies. Indeed, most reported SQ dyes are either non-emissive or their fluorescence was not measured, which might impede direct comparisons with experiment (no AFCP is available by definition), an aspect that is treated in the following. Our results are listed in Table 1, that also reports the mean signed error (MSE), mean absolute error (MAE) and the linear correlation coefficient obtained from a least-square fit between theory and experiment (R). Obviously, the TD-DFT 0-0 energies are systematically too large, with an average deviation exceeding 0.40 eV. This overestimation was already reported previously for SQ derivatives [40,44,46], and is

therefore related to the limitations of TD-DFT rather than to the specific form of the selected XCF. This large positive MSE is symptomatic of a large reorganization of the electron density when going from the GS to the ES (see Fig. 1), as was demonstrated previously in the cases of merocyanine derivatives and BODIPY dyes [41,77–79], two classes of dyes that do not imply significant CT. When applying the SOS-CIS(D) method to determine the transition energies on the DFT/TD-DFT structures, a strong downshift of the transition energies is obtained (by more than half an eV on average) and this leads to an underestimation of the experimental 0-0 energies by more than 0.15 eV with only a very slight improvement in the theory/experiment correlation. While the SOS-CIS(D) MAE is clearly more satisfying than its TD-DFT counterpart, it remains significant for a wavefunction approach partially accounting for the impact of double excitations on the ES properties. We recall here that SOS-CIS(D) was found particularly effective for fluoroborate emitters [69]. Clearly, the ADC(2) values are the most accurate in the present case with an average error of 0.11 eV (small underestimation of the experimental value) and the largest correlation with the experimental values.

Given that is it difficult to compare 0-0 energies to AFCP if no emission was measured, which approximation is best suited to evaluate the experimental values? To answer this question, let us first remind that the theoretical 0-0 energies have been determined as:

$$E^{0-0} = E^{\text{adia}} + \Delta E^{\text{ZPVE}} \quad (1)$$

where E^{adia} is the adiabatic energy, that is the difference between the ES and GS total energies determined at their respective minima and ΔE^{ZPVE} is the difference between the ES and GS ZPVE energies. Clearly, the first term in this equation is dominating and one could be tempted to neglect altogether the second term that is both smaller and more difficult to compute. For the molecules listed in Table 1, this would lead to an average increase of the theoretical energies by 0.048 eV. We note that this increase is rather small compared to the results obtained for other organic compounds where the typical ΔE^{ZPVE} is closer to ca. -0.080 eV [54,55]. As a second approximation, one could directly use theoretical vertical absorption energies instead of adiabatic energies in the comparisons. This means that one would consider the difference between ES and GS energies determined on the optimal GS geometry only, making the calculation of the ES geometry useless. Such approximation is common as it considerably fasten the calculations and it



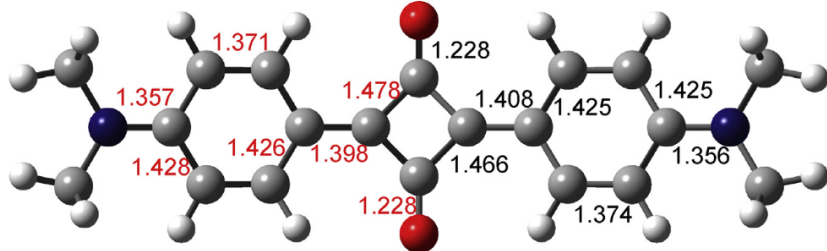
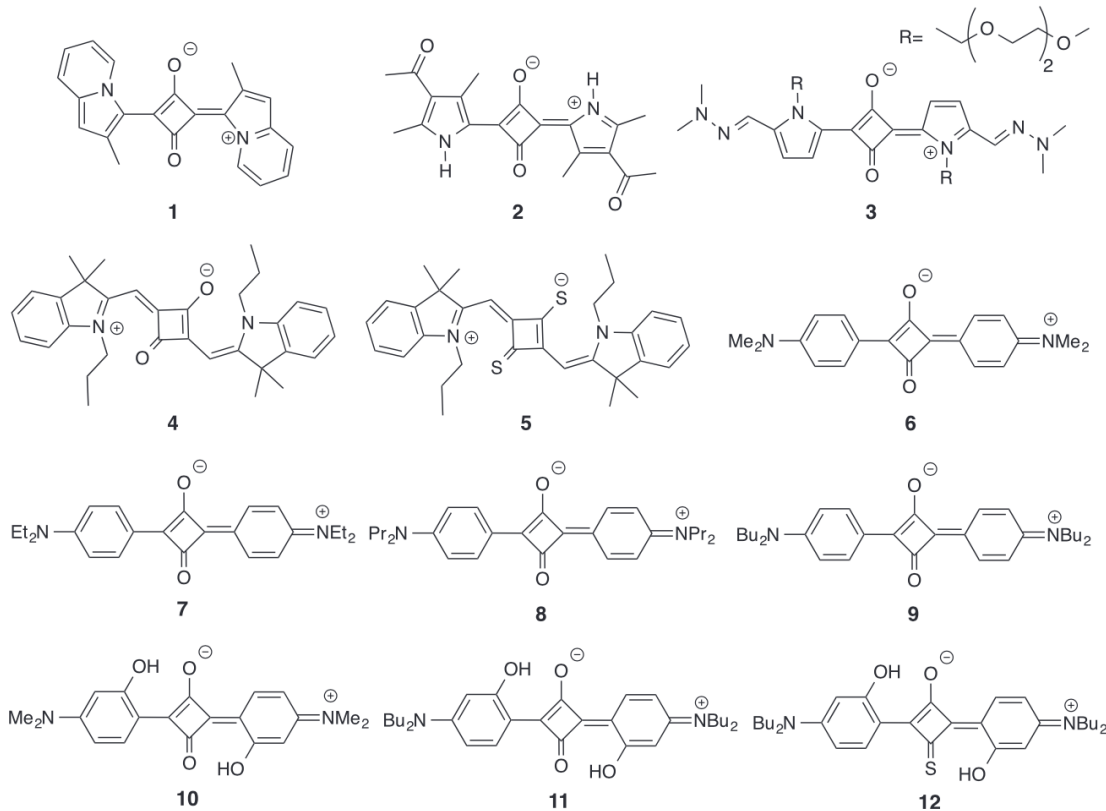


Fig. 2. Selected (TD-)DFT bond lengths for the GS (in black, on the r.h.s.) and ES (in red on the l.h.s.) for one of the two dyes represented in Fig. 1. (For interpretation of the references to colour in this figure legend, the reader is referred to the web version of this article.)



Scheme 1. Representation of the 12 SQs for which comparisons between experimental and theoretical 0-0 energies have been carried out.

was indeed widely applied for SQs previously (see Introduction). Doing such “vertical” approximation further increases the computed transition energies by 0.035 eV, 0.061 eV and 0.071 eV, on average with TD-DFT, SOS-CIS(D) and ADC(2), respectively. These variations are not drastic but are nevertheless significant, especially for the two wavefunction theories. These values also illustrate that, on the one hand, wavefunction transition energies are more sensitive than their TD-DFT counterparts to the geometry, and, on the other hand, that applying the vertical approximation comes with a significant cost in terms of accuracy. Interestingly, if one compares directly the ADC(2) vertical absorption energies to the experimental AFCP, one obtains MSE and MAE as small as –0.003 eV and 0.056 eV, respectively, but this success is clearly due to fortuitous cancellations of errors. In short, neglecting both

very small, the measured longest wavelength of maximal absorption, λ_{\max} , is only slightly above the experimental AFCP on the energy scale. Indeed, for the 12 compounds of Table 1, the average shift is 0.02 eV only. In other words, considering the measured λ_{\max} as the experimental 0-0 energy is a “better” approximation than simplifying the theoretical protocol by neglecting vibrational or geometrical differences between the two states.

Lets us now turn towards the band shapes determined for selected SQs. As shown on Fig. 3 for 4 and 5, the topologies of both absorption and fluorescence spectra are well reproduced using the TD-DFT vibronic couplings computed in the harmonic approximation. For instance, the compound 5 in which the oxygen atoms of the SQ core have been substituted by sulfur atoms exhibit broader band than 4, which is consistent with experiment. The SQs ab-

Table 1

Comparison between experimental and theoretical 0-0 energies computed at several levels of theories. All values are in eV. The SOS-CIS(D) and ADC(2) values have been determined using the TD-DFT structures and vibrational energies (See Ref. [60]). At the bottom of the Table, we report statistical data for this set of compounds mean signed error (MSE), mean absolute error (MAE) and linear correlation coefficient (R).

Molecule	Solvent	Exp.	TD-DFT	SOS-CIS(D)	ADC(2)
1	CH ₂ Cl ₂	1.793 [80]	2.133	1.539	1.694
2	CH ₂ Cl ₂	2.157 [81]	2.526	2.007	2.117
3	CH ₂ Cl ₂	1.761 [80]	2.097	1.634	1.678
4	CH ₂ Cl ₂	1.940 [82]	2.320	1.704	1.754
5	Toluene	1.811 [82]	2.109	1.540	1.620
6	CH ₂ Cl ₂	1.935 [83,84]	2.420	1.877	1.898
7	CH ₂ Cl ₂	1.931 [83]	2.381	1.823	1.837
8	CH ₂ Cl ₂	1.923 [83]	2.368	1.811	1.820
9	Toluene	1.934 [82]	2.354	1.803	1.800
10	CH ₂ Cl ₂	1.917 [84]	2.410	1.773	1.838
11	CH ₂ Cl ₂	1.896 [82]	2.364	1.721	1.769
12	CH ₃ CN	1.864 [82]	2.291	1.681	1.732
MSE			0.409	-0.162	-0.109
MAE			0.409	0.162	0.109
R			0.893	0.895	0.936

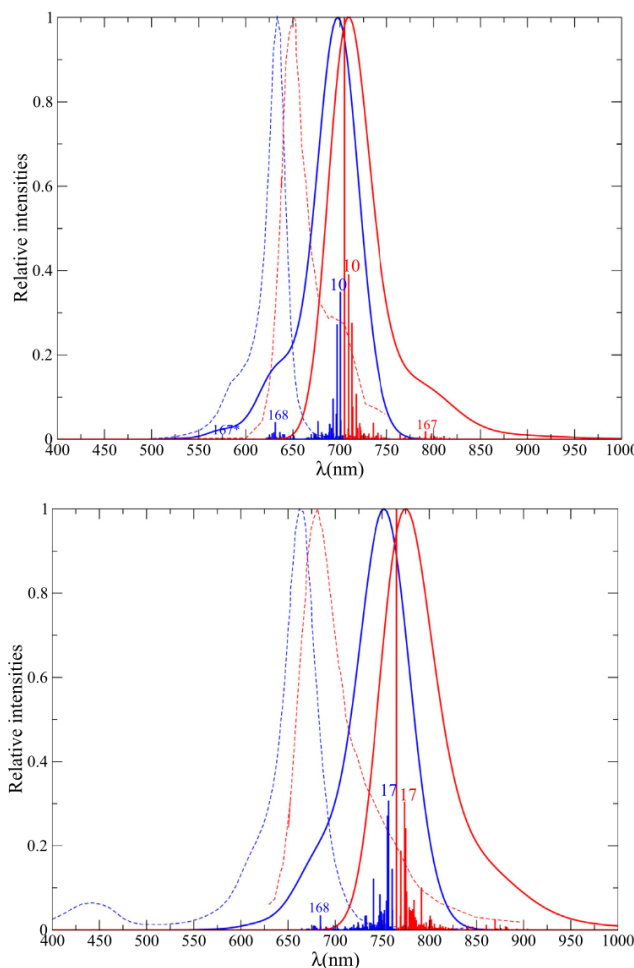


Fig. 3. Comparison between the experimental (dashed) and theoretical (full) absorption (blue) and emission (red) vibrationally resolved bands for **4** (left) and **5**. The experimental graphs are adapted from Ref. [82]. The 0-0 energies are the one obtained

This mode (10 and 17 in **4** and **5**, respectively) modifies the N-H ... X hydrogen bond length and appears at low frequency (88 and 143 cm⁻¹ for **4** and **5** depicted on Fig. 3, see the SI for representation). The shoulder present in both **4** to **5** is related to a symmetric C-C stretching mode inducing a breathing of the SQ core (mode 168 in both dyes, see Fig. 3). This mode takes place at 1648 cm⁻¹ in **4** and 1546 cm⁻¹ in **5** (see the SI). For the former dye, a second important mode (mode 167 at 1617 cm⁻¹), which is asymmetric, also plays a role in the band shapes of the absorption. In the fluorescence spectra the breathing mode only appears to be important for the a hump in **4** and not in **5**. Likewise, a good agreement between theoretical and experimental band shapes was also obtained for compound **2** (see the SI).

3.3. Comparisons with experimental λ_{max}

Given the conclusions obtained in the previous Section, we have established a set of 39 SQ derivatives and compared the theoretical 0-0 energies to the experimental λ_{max} . Raw data as well as representation of all treated compounds can be found in the SI, whereas the results are graphically summarized in Fig. 4. This figure shows that the previously reported trends pertain. Indeed, TD-DFT overestimates considerably the experimental values whereas the two wavefunction methods yield the opposite error though with a smaller magnitude. Indeed, the MSE (MAE) attains 0.363 (0.363) eV, -0.180 (0.180) eV and -0.124 (0.125) eV for TD-DFT, SOS-CIS(D) and ADC(2), respectively. The correlation between experimental and theoretical values are in the 0.91–0.94 range for the three methods.

4. Conclusions

We have modeled the ground and excited electronic states of the largest panel of SQ derivatives considered to date with *ab initio* approaches. This is also the first theoretical investigation to obtain 0-0 energies for this class of molecules, therefore paving the way to more meaningful theory-experiment comparisons. We concluded

Theory (eV)

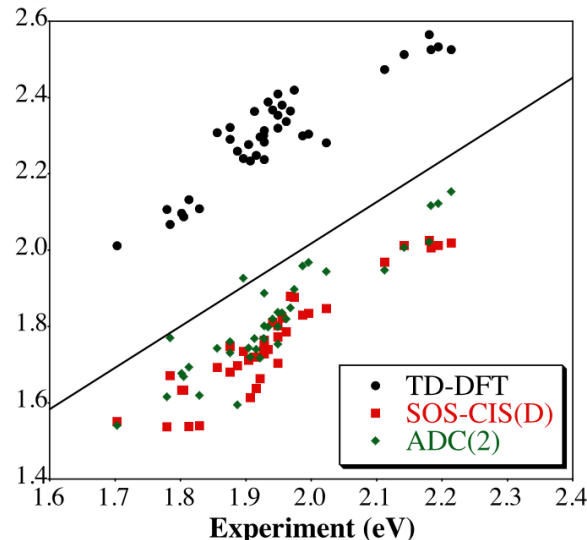


Fig. 4. Comparison between the experimental λ_{max} and the theoretical 0-0 energies

that these dyes present mainly features consistent with a cyanine like nature. Indeed, we found: i) a strong reorganization of the electron density with alternating losses/gains of electrons on the odd/even atoms constituting the π -conjugated path; ii) rather small geometric changes when going from the GS to the ES, the largest variations being localized on the SQ carbon core, the CO distance remaining almost constant upon electronic transition; iii) TD-DFT transition energies that are significantly too large compared to experiment. To obtain accurate 0–0 energies, one can correct the TD-DFT values by the adiabatic transition energies determined at the ADC(2) level. In such computationally efficient protocol, the structural and vibrational parameters are computed with (TD-)DFT, the solvent effects are accounted for by the PCM continuum model and only the transition energies (absorption, emission, adiabatic) are determined at the wavefunction level. This allows to reproduce the experimental values with a ca. 0.11 eV accuracy. We have also showed that using vertical theoretical absorption energies or neglecting the difference between the zero-point energies of the two states may yield significant deviations compared to the 0–0 energies. In contrast, using the experimental λ_{max} as an estimate of the AFCP energy is a more valuable approximation. Besides, the band shapes obtained on the basis of the TD-DFT vibrational spectra of the ground- and excited-states are in good agreement with experiment confirming that the TD-DFT structures are indeed rather accurate. These vibronic calculations also demonstrated that the vibrational mode deforming the central square cycle is responsible for the presence of a shoulder in the experimental spectra.

Acknowledgements

D.J. acknowledges the European Research Council (ERC) for financial support in the framework of a Starting Grant (Marches - 278845). This research used resources of 1) the GENCI-CINES/IDRIS, 2) the CCIPL (*Centre de Calcul Intensif des Pays de Loire*) and 3) a local Troy cluster.

Appendix A. Supplementary data

Supplementary data related to this article can be found at <http://dx.doi.org/10.1016/j.dyepig.2016.11.046>.

References

- [1] Meier H, Dullweber U. Bis(stilbenyl)squaraines — novel pigments with extended conjugation. *Tetrahedron Lett* 1996;37(8):1191–4. [http://dx.doi.org/10.1016/0040-4039\(95\)02414-X](http://dx.doi.org/10.1016/0040-4039(95)02414-X).
- [2] Meier H, Dullweber U. Extension of the squaraine chromophore in symmetrical bis(stilbenyl)squaraines. *J Org Chem* 1997;62(14):4821–6. <http://dx.doi.org/10.1021/jo970284e>.
- [3] Meier H, Petermann R. Near infrared dyes by combination of squaraine and ferrocene chromophores. *Tetrahedron Lett* 2000;41(29):5475–8. [http://dx.doi.org/10.1016/S0040-4039\(00\)00892-3](http://dx.doi.org/10.1016/S0040-4039(00)00892-3).
- [4] Nizomov N, Ismailov ZF, Nizamov SN, Salakhiddinova MK, Tatarets AL, Patseker LD, et al. Spectral-luminescent study of interaction of squaraine dyes with biological substances. *J Mol Struct* 2006;788(1–3):36–42. <http://dx.doi.org/10.1016/j.molstruc.2005.11.014>.
- [5] Ros-Lis J, Martínez-Máñez R, Sancenón F, Soto J, Spieles M, Rurack K. Squaraines as reporter units: insights into their photophysics, protonation, and metal-ion coordination behaviour. *Chem Eur J* 2008;14(32):10101–14. <http://dx.doi.org/10.1002/chem.200800300>.
- [6] Sreejith S, Carol P, Chithra P, Ajayaghosh A. Squaraine dyes: a mine of molecular materials. *J Mater Chem* 2008;18:264–74. <http://dx.doi.org/10.1039/B707734C>.
- [7] Beverina L, Salice P. Squaraine compounds: tailored design and synthesis towards a variety of material science applications. *Eur J Org Chem* 2010;2010:731–1207. <http://dx.doi.org/10.1002/ejoc.200900707>
- [9] Marks P, Levine M. Synthesis of a near-infrared emitting squaraine dye in an undergraduate organic laboratory. *J Chem Educ* 2012;89(9):1186–9. <http://dx.doi.org/10.1021/ed300187d>.
- [10] Rao BA, Kim H, Son Y-A. Synthesis of near-infrared absorbing pyrylium-squaraine dye for selective detection of hg^{2+} . *Sens Actuat B Chem* 2013;188:847–56. <http://dx.doi.org/10.1016/j.snb.2013.07.073>.
- [11] Hu L, Yan Z, Xu H. Advances in synthesis and application of near-infrared absorbing squaraine dyes. *RSC Adv* 2013;3:7667–76. <http://dx.doi.org/10.1039/C3RA23048A>.
- [12] Sleiman MH, Ladame S. Synthesis of squaraine dyes under mild conditions: applications for labelling and sensing of biomolecules. *Chem Commun* 2014;50:5288–90. <http://dx.doi.org/10.1039/C3CC47894G>.
- [13] Beverina L, Sassi M. Twists and turns around a square: the many faces of squaraine chemistry. *Synlett* 2014;25(4):477–90.
- [14] Lynch DE. Pyrrolyl squaraines—fifty golden years. *Metals* 2015;5(3):1349. <http://dx.doi.org/10.3390/met5031349>.
- [15] Pascal S, Haefele A, Monnereau C, Charaf-Eddin A, Jacquemin D, Le Guennic B, et al. Expanding the polymethine paradigm: evidence for the contribution of a bis-dipolar electronic structure. *J Phys Chem A* 2014;118(23):4038–47. <http://dx.doi.org/10.1021/jp501358q>.
- [16] Luo S, Zhang E, Su Y, Cheng T, Shi C. A review of nir dyes in cancer targeting and imaging. *Biomaterials* 2011;32(29):7127–38. <http://dx.doi.org/10.1016/j.biomaterials.2011.06.024>.
- [17] Gao F-P, Lin Y-X, Li L-L, Liu Y, Mayerhöffer U, Spenst P, et al. Upromolecular adducts of squaraine and protein for non- invasive tumor imaging and photothermal therapy *in vivo*. *Biomaterials* 2014;35(3):1004–14. <http://dx.doi.org/10.1016/j.biomaterials.2013.10.039>.
- [18] Imazawa K, Citterio D, Suzuki K. New trends in near-infrared fluorophores for bioimaging. *Anal Sci* 2014;30(3):327–49. <http://dx.doi.org/10.2116/analsci.30.327>.
- [19] Ramaiyah D, Eckert I, Arun KT, Weidenfelder L, Epe B. Squaraine dyes for photodynamic therapy: study of their cytotoxicity and genotoxicity in bacteria and mammalian cells. *Photochem Photobiol* 2002;76(6):672–7. [http://dx.doi.org/10.1562/0031-8655\(2002\)0760672SDFTS2.0.CO.2](http://dx.doi.org/10.1562/0031-8655(2002)0760672SDFTS2.0.CO.2).
- [20] Ramaiyah D, Eckert I, Arun KT, Weidenfelder L, Epe B. Squaraine dyes for photodynamic therapy: mechanism of cytotoxicity and dna damage induced by halogenated squaraine dyes plus light (>600 nm). *Photochem Photobiol* 2004;79(1):99–104. <http://dx.doi.org/10.1111/j.1751-1097.2004.tb09863.x>.
- [21] Santos P, Reis L, Almeida P, Serrano J, Oliveira A, Ferreira LV. Efficiency of singlet oxygen generation of aminosquarylium cyanines. *J Photochem Photobiol A* 2004;163(1–2):267–9. <http://dx.doi.org/10.1016/j.jphotochem.2003.12.007>.
- [22] Avirah RR, Jayaram DT, Adarsh N, Ramaiyah D. Squaraine dyes in pdt: from basic design to *in vivo* demonstration. *Org Biomol Chem* 2012;10:911–20. <http://dx.doi.org/10.1039/C1OB06588B>. URL.
- [23] Abrahamse H, Hamblin MR. New photosensitizers for photodynamic therapy. *Biochem J* 2016;473(4):347–64. <http://dx.doi.org/10.1042/BJ20150942>.
- [24] Serpe L, Ellena S, Barbera N, Foglietta F, Prandini F, Gallo MP, et al. Squaraines bearing halogenated moieties as anticancer photosensitizers: synthesis, characterization and biological evaluation. *Eur J Med Chem* 2016;113:187–97. <http://dx.doi.org/10.1016/j.ejmchem.2016.02.035>.
- [25] Jayaram DT, Ramos-Romero S, Shankar BH, Garrido C, Rubio N, Sanchez-Cid L, et al. In vitro and *in vivo* demonstration of photodynamic activity and cytoplasm imaging through tpe nanoparticles. *ACS Chem Biol* 2016;11(1):104–12. <http://dx.doi.org/10.1021/acschembio.5b00537>.
- [26] Hwang SH, Kim NK, Koh KN, Kim SH. Absorption spectra and electrophotographic properties of squarylium dyes containing a nitro group. *Dyes Pigm* 1998;39(4):359–69. [http://dx.doi.org/10.1016/S0143-7208\(98\)00021-7](http://dx.doi.org/10.1016/S0143-7208(98)00021-7).
- [27] Tian M, Furuki M, Iwasa I, Sato Y, Pu LS, Tatsuzawa S. Search for squaraine derivatives that can be sublimed without thermal decomposition. *J Phys Chem B* 2002;106(17):4370–6. <http://dx.doi.org/10.1021/jp013698r>.
- [28] Mori T, Kim H-G, Mizutani T, Lee D-C. Electroluminescent properties in organic light-emitting diode doped with two guest dyes. *Jpn J Appl Phys* 2001;40(9R):5346. URL, <http://stacks.iop.org/1347-4065/40/i=9R/a=5346>.
- [29] Mazzeo M, Genco A, Gambino S, Ballarini D, Mangione F, Di Stefano O, et al. Ultrastrong light-matter coupling in electrically doped microcavity organic light emitting diodes. *Appl Phys Lett* 2014;104(23). <http://dx.doi.org/10.1063/1.4882422>.
- [30] Anees P, Sreejith S, Ajayaghosh A. Self-assembled near-infrared dye nanoparticles as a selective protein sensor by activation of a dormant fluorophore. *J Am Chem Soc* 2014;136(38):13233–9. <http://dx.doi.org/10.1021/ja503850b>.
- [31] Gale PA, Caltagirone C. Anion sensing by small molecules and molecular ensembles. *Chem Soc Rev* 2015;44:4212–27. <http://dx.doi.org/10.1039/C4CS00179F>.
- [32] Chen G, Sasabe H, Sasaki Y, Katagiri H, Wang X-F, Sano T, et al. A series of squaraine dyes: effects of side chain and the number of hydroxyl groups on material properties and photovoltaic performance. *Chem Mater* 2014;26(3):1356–64. <http://dx.doi.org/10.1021/cm4034929>.
- [33] An Q, Zhang F, Li L, Wang J, Zhang J, Zhou L, et al. Improved efficiency of bulk heterojunction polymer solar cells by doping low-bandgap small molecules. *ACS Appl Mat Int* 2014;6(9):6537–44. <http://dx.doi.org/10.1021/am500074e>

- Cooperative enhancement versus additivity of two-photon-absorption cross sections in linear and branched squaraine superchromophores. *Phys Chem Chem Phys* 2016;18:16404–13. <http://dx.doi.org/10.1039/C6CP02312F>.
- [36] Liu T, Bondar MV, Belfield KD, Anderson D, Masunov AE, Hagan DJ, et al. Linear photophysics and femtosecond nonlinear spectroscopy of a star-shaped squaraine derivative with efficient two-photon absorption. *J Phys Chem C* 2016;120(20):11099–110. <http://dx.doi.org/10.1021/acs.jpcc.6b02446>.
- [37] Ballesteros-Barrientos AR, Woodward AW, Moreshead WV, Bondar MV, Belfield KD. Synthesis and linear and nonlinear photophysical characterization of two symmetrical pyrene-terminated squaraine derivatives. *J Phys Chem C* 2016;120(14):7829–38. <http://dx.doi.org/10.1021/acs.jpcc.6b00143>.
- [38] Bigelow RW, Freund H-J. An mndo and cndo/s(s + des ci) study on the structural and electronic properties of model squaraine dye and related cyanine. *Chem Phys* 1986;107(2):159–74. [http://dx.doi.org/10.1016/0301-0104\(86\)85001-7](http://dx.doi.org/10.1016/0301-0104(86)85001-7).
- [39] Geiger T, Kuster S, Yum J-H, Moon S-J, Nazeeruddin MK, Grätzel M, et al. Molecular design of unsymmetrical squaraine dyes for high efficiency conversion of low energy photons into electrons using TiO_2 nanocrystalline films. *Adv Func Mater* 2009;19(17):2720–7. <http://dx.doi.org/10.1002/adfm.200900231>.
- [40] Quartarolo AD, Sicilia E, Russo N. On the potential use of squaraine derivatives as photosensitizers in photodynamic therapy: a tddft and ricc2 survey. *J Chem Theory Comput* 2009;5(7):1849–57. <http://dx.doi.org/10.1021/ct900199j>.
- [41] Le Guennic B, Jacquemin D. Taking up the cyanine challenge with quantum tools. *Acc Chem Res* 2015;48:530–7. <http://dx.doi.org/10.1021/ar500447q>.
- [42] Tozer DJ. Relationship between long-range charge-transfer excitation energy error and integer discontinuity in kohn-sham theory. *J Chem Phys* 2003;119:12697–9.
- [43] Drew A, Head-Gordon M. Failure of time-dependent density functional theory for long-range charge-transfer excited states: the zincbacteriochlorin-bacteriochlorin and bacteriochlorophyll-spheroide complexes. *J Am Chem Soc* 2004;126:4007–16.
- [44] Alberto ME, Mazzone G, Quartarolo AD, Fortes Ramos Sousa F, Sicilia E, Russo N. Electronic spectra and intersystem spin-orbit coupling in 1,2- and 1,3-squaraines. *J Comput Chem* 2014;35(29):2107–13. <http://dx.doi.org/10.1002/jcc.23725>.
- [45] Ronchi E, Ruffi R, Rizzato S, Albinati A, Beverina L, Pagani GA. Regioselective synthesis of 1,2- vs 1,3-squaraines. *Org Lett* 2011;13(12):3166–9. <http://dx.doi.org/10.1021/ol201093t>.
- [46] Krishna Chaitanya G, Puyad AL, Bhanuprakash K. Charge transfer or biradicaloid character: assessing td-dft and sac-ci for squarylium dye derivatives. *RSC Adv* 2015;5:18813–21. <http://dx.doi.org/10.1039/C4RA10649K>.
- [47] Liu X, Cho B, Chan L-Y, Kwan WL, Ken Lee C-L. Development of asymmetrical near infrared squaraines with large stokes shift. *RSC Adv* 2015;5:106868–76. <http://dx.doi.org/10.1039/C5RA18998E>.
- [48] Xu J, Zhang H, Wang L, Liang G, Wang L, Shen X, et al. Dft and td-dft studies on symmetrical squaraine dyes for nanocrystalline solar cells. *Monatsh Chem* 2010;141(5):549–55. <http://dx.doi.org/10.1007/s00706-010-0298-0>.
- [49] Prostota Y, Kachkovsky OD, Reis LV, Santos PF. New unsymmetrical squaraine dyes derived from imidazo[1,5-a]pyridine. *Dyes Pigm* 2013;96(2):554–62. <http://dx.doi.org/10.1016/j.dyepig.2012.10.006>.
- [50] El-Shishtawy RM, Elroby SA, Asiri AM, Hilal RH. Pyran-squaraine as photosensitizers for dye-sensitized solar cells: Dft/tddft study of the electronic structures and absorption properties. *Int J Photoenergy* 2014;136893.
- [51] Maltese V, Cospito S, Beneduci A, De Simone BC, Russo N, Chidichimo G, et al. Electro-optical properties of neutral and radical ion thienosquaraines. *Chem Eur J* 2016;22(29):10179–86. <http://dx.doi.org/10.1002/chem.201601281>.
- [52] Santoro F, Jacquemin D. Going beyond the vertical approximation with time-dependent density functional theory. *WIREs Comput Mol Sci* 2016;6(5):460–86. <http://dx.doi.org/10.1002/wcms.1260>.
- [53] Avila Ferrer FJ, Cerezo J, Stendardo E, Impronta R, Santoro F. Insights for an accurate comparison of computational data to experimental absorption and emission spectra: beyond the vertical transition approximation. *J Chem Theory Comput* 2013;9:2072–82.
- [54] Goerigk L, Grimm S. Calculation of electronic circular dichroism spectra with time-dependent double-hybrid density functional theory. *J Phys Chem A* 2009;113(4):767–76. <http://dx.doi.org/10.1021/jp807366r>.
- [55] Jacquemin D, Planchat A, Adamo C, Mennucci B. A td-dft assessment of functionals for optical 0-0 transitions in solvated dyes. *J Chem Theory Comput* 2012;8:2359–72.
- [56] Tomasi J, Mennucci B, Cammi R. Quantum mechanical continuum solvation models. *Chem Rev* 2005;105:2999–3094.
- [57] Caricato M, Mennucci B, Tomasi J, Ingrosso F, Cammi R, Corni S, et al. Formation and relaxation of excited states in solution: a new time dependent polarizable continuum model based on time dependent density functional theory. *J Chem Phys* 2006;124:124520.
- [58] Drew A, Wormit M. The algebraic diagrammatic construction scheme for the polarization propagator for the calculation of excited states. *WIREs Comput Mol Sci* 2015;5(1):82–95. <http://dx.doi.org/10.1002/wcms.1206>.
- [59] Head-Gordon M, Maurice D, Oumi M. A perturbative correction to restricted non-collinear configuration interaction with single substitutions for excited-state calculations. *J Chem Theory Comput* 2013;9:2072–82.
- [60] Frisch MJ, Trucks GW, Schlegel HB, Scuseria GE, Robb MA, Cheeseman JR, et al. Gaussian 09 revision D.01. Gaussian Inc. Wallingford CT; 2009.
- [61] Zhao Y, Truhlar DG. Density functionals with broad applicability in chemistry. *Acc Chem Res* 2008;41:157–67.
- [62] Zhao Y, Truhlar DG. The m06 suite of density functionals for main group thermochemistry, thermochemical kinetics, noncovalent interactions, excited states, and transition elements: two new functionals and systematic testing of four m06-class functionals and 12 other functionals. *Theor Chem Acc* 2008;120:215–41.
- [63] Leang SS, Zahariev F, Gordon MS. Benchmarking the performance of time-dependent density functional methods. *J Chem Phys* 2012;136:104101.
- [64] Isegawa M, Peverati R, Truhlar DG. Performance of recent and high-performance approximate density functionals for time-dependent density functional theory calculations of valence and rydberg electronic transition energies. *J Chem Phys* 2012;137:244104.
- [65] Charaf-Eddin A, Planchat A, Mennucci B, Adamo C, Jacquemin D. Choosing a functional for computing absorption and fluorescence band shapes with td-dft. *J Chem Theory Comput* 2013;9:2749–60. <http://dx.doi.org/10.1021/ct4000795>.
- [66] Cammi R, Mennucci B. The linear response theory for the polarizable continuum model. *J Chem Phys* 1999;110:9877–86.
- [67] Cossi M, Barone V. Time-dependent density functional theory for molecules in liquid solutions. *J Chem Phys* 2001;115:4708–17.
- [68] Chibani S, Laurent AD, Le Guennic B, Jacquemin D. Improving the accuracy of excited state simulations of bodipy and aza-bodipy dyes with a joint sos-cis(d) and td-dft approach. *J Chem Theory Comput* 2014;10:4574–82.
- [69] Turbomole v6.6 2014, a development of university of karlsruhe and forschungszentrum karlsruhe gmbh, 1989–2007, turbomole gmbh, since 2007; Available from: <http://www.turbomole.com> (Accessed 13 June 2016).
- [70] Shao Y, Gan Z, Epifanovsky E, Gilbert AT, Wormit M, Kussmann J, et al. Advances in molecular quantum chemistry contained in the q-chem 4 program package. *Mol Phys* 2015;113:184–215. <http://dx.doi.org/10.1080/00268976.2014.952696>.
- [71] Laurent A, Blondel A, Jacquemin D. Choosing an atomic basis set for td-dft, soppa, adc(2), cis(d), cc2 and eom-ccsd calculations of low-lying excited states of organic dyes. *Theor Chem Acc* 2015;134(6):76. <http://dx.doi.org/10.1007/s00214-015-1676-9>.
- [72] Santoro F, Impronta R, Lami A, Bloino J, Barone V. Effective method to compute franck-condon integrals for optical spectra of large molecules in solution. *J Chem Phys* 2007;126:084509.
- [73] Santoro F, Impronta R, Lami A, Bloino J, Barone V. Effective method to compute vibrationally resolved optical spectra of large molecules at finite temperature in the gas phase and in solution. *J Chem Phys* 2007;126:184102.
- [74] Santoro F, Impronta R, Lami A, Bloino J, Barone V. Effective method for the computation of optical spectra of large molecules at finite temperature including the duschinsky and herzberg-teller effect: the qx band of porphyrin as a case study. *J Chem Phys* 2008;128:224311.
- [75] Masunov AE. Theoretical spectroscopy of carbocyanine dyes made accurate by frozen density correction to excitation energies obtained by td-dft. *Int J Quantum Chem* 2010;110:3095–100.
- [76] Send R, Valsson O, Filippi C. Electronic excitations of simple cyanine dyes: reconciling density functional and wave function methods. *J Chem Theory Comput* 2011;7(2):444–55.
- [77] Moore II B, Autschbach J. Longest-wavelength electronic excitations of linear cyanines: the role of electron delocalization and of approximations in time-dependent density functional theory. *J Chem Theory Comput* 2013;9:4991–5003. <http://dx.doi.org/10.1021/ct400649r>.
- [78] Zhukova H, Krykunov M, Autschbach J, Ziegler T. Applications of time dependent and time independent density functional theory to the first π to π^* transition in cyanine dyes. *J Chem Theory Comput* 2014;10:3299–307.
- [79] Behera L, Abbott A, Landenna M, Cerninara M, Tubino R, Meinardi F, et al. New -extended water-soluble squaraines as singlet oxygen generators. *Org Lett* 2005;7(19):4257–60. <http://dx.doi.org/10.1021/oj0516871>.
- [80] Patrick B, George MV, Kamat PV, Das S, Thomas KG. Photochemistry of squaraine dyes: excited states and reduced and oxidized forms of 4-(4-acetyl-3,5-dimethylpyrrolidin-2-ylidene)-2-(4-acetyl-3,5-dimethylpyrrol-2-yl)-3-oxocyclobut-1-en-1-olate. *J Chem Soc Faraday Trans* 1992;88:671–6. <http://dx.doi.org/10.1039/FT9928800671>.
- [81] Peclci D, Hu H, Fishman DA, Webster S, Przhonska OV, Kurdyukov VV, et al. Enhanced intersystem crossing rate in polymethine-like molecules: sulfur-containing squaraines versus oxygen-containing analogues. *J Phys Chem A* 2013;117(11):2333–46. <http://dx.doi.org/10.1021/jp400276g>.
- [82] Law KY. Squaraine chemistry: effects of structural changes on the absorption and multiple fluorescence emission of bis[4-(dimethylamino)phenyl]squaraine and its derivatives. *J Phys Chem* 1987;91(20):5184–93. <http://dx.doi.org/10.1021/j100304a012>.
- [83] Kamat PV, Das S, Thomas KG, George MV. Photochemistry of squaraine dyes. 1. excited singlet, triplet, and redox states of bis[4-(dimethylamino)phenyl]squaraine and bis[4-(dimethylamino)-2-hydroxybenzyl]squaraine. *J Phys Chem* 1990;94(10):4533–40. <http://dx.doi.org/10.1021/j100304a012>.
- [84] Head-Gordon M, Maurice D, Oumi M. A perturbative correction to restricted non-collinear configuration interaction with single substitutions for excited-state calculations. *J Chem Theory Comput* 2013;9:2072–82.

open shell conformation interaction with single substitutions for excited states of radicals. *Chem Phys Lett* 1995;246:114–21.

Squaraine and bis[4-(dimethylamino)-2-hydroxyphenyl]squaraine. *J Phys Chem* 1992;96(1):195–9. <http://dx.doi.org/10.1021/j100180a038>.

- [60] Jacquemin D, Duchemin I, Blase X. 0-0 energies using hybrid schemes: